Applied Surface Science 456 (2018) 147–155

Contents lists available at ScienceDirect

Applied Surface Science

journal homepage: www.elsevier.com/locate/apsusc

Full Length Article

The influence of alumina nanoparticles on lattice defects, crystallographic texture and residual stresses in electrodeposited Ni/Al_2O_3 composite coatings

Anna Góral[a,*], Stanisław J. Skrzypek[b]

[a] Institute of Metallurgy and Materials Science, Polish Academy of Sciences, Reymonta 25, 30-059 Kraków, Poland
[b] Faculty of Metals Engineering and Industrial Computer Science, AGH University of Science and Technology, Av. Mickiewicza 30, 30-059 Kraków, Poland

ARTICLE INFO

Keywords:
Ni/Al_2O_3 coating
Electrodeposition
Nanocomposite
Residual stresses
Crystallographic texture

ABSTRACT

This paper presents how various additions of Al_2O_3 nanoparticles in the electrolytic bath modified the Ni/Al_2O_3 nanocomposite coating microstructure. The residual stresses, lattice defects, and crystallographic texture of the obtained deposits were studied. The investigations showed that the tensile residual stresses corresponded to the ceramic nanoparticles content in the deposited coating. The high level of measured stresses in the Ni/Al_2O_3 coatings indicated the presence of strengthening mechanisms caused by the Al_2O_3 nanoparticles. The density of crystal lattice defects and grain refinement contributed to the strengthening of the Ni matrix. The main texture components and lattice parameters were more sensitive to deposit thickness changes than to the amount of alumina nanoparticles embedded in the coatings. The Ni/Al_2O_3 with the smallest thickness showed the highest lattice parameters of the Ni matrix.

1. Introduction

Surface layers and coatings are important in various applications due to their specific properties, compared to bulk materials, and they provide components with higher qualities and longer lifetime. These characteristics concern physical, chemical, mechanical and tribological properties [1–8]. Electrodeposited nickel composite coatings are usually applied in industrial environments due to their excellent corrosion and wear resistance, as well as other functional properties like thermal and electrical conducting [9–12]. They may be used in high temperature braizing and as coatings of powders for better sintering. Ni/Al_2O_3 composite coatings can be used as high-wear resistance deposits. They may be applied in roll forming industry for production such parts as bearing [13]. Nowadays, electrodeposition also allows to produce nanocomposite coatings with improved overall performance. This process is conducted in an electrolytic solution, in which insoluble hard nanoparticles are suspended. By stirring the solution bath during the process the particles are embedded in the metal matrix. Among others, functional properties of electrodeposited composites depend strongly on their microstructure (phase composition, grain size, and lattice defects), residual stresses and texture (distribution of crystallographic orientations). Although many research studies have been focused on Ni/Al_2O_3 composite coatings [7,9,14–16], there is lack of correlation between the microstructure, residual stresses and manufacturing process parameters. The residual stresses that occur in the deposits have a significant influence on their properties [17,18]. El-Sherik et al. [19] reported three kinds of residual stresses which exist in plated coatings: (1) lattice misfit stresses, resulting from distortion due to differences in lattice parameters at the interface between the coating and substrate, (2) thermal stresses arising due to differences in thermal coefficient of expansion at the interface between the substrate and coating, and (3) stress that results from particular plating conditions and bath composition. In the electrodeposited pure Ni, Ni alloyed and composite coatings mainly tensile residual stresses were observed [7,20–24]. There are no studies on the influence of lattice defects and crystallographic texture on residual stresses in electrodeposited coatings. Little attention has been paid so far to researching the effects of the amounts of Al_2O_3 nanoparticles introduced into the electrolytic bath on the coatings' residual stress state. Moreover, the character of residual stresses (tensile, compressive) was found to be different depending on the bath composition and deposition parameters [7,19,20]. Góral et al. and Erler et al. [7,20] reported tensile residual stresses in Ni/Al_2O_3 coatings, whereas El-Sherik et al. [19] presented compressive stresses.

The aim of this paper is to investigate how Al_2O_3 nanoparticles affect crystal lattice defects, crystallographic texture and residual stresses in the electrodeposited Ni/Al_2O_3 nanocomposite coatings. The

* Corresponding author.
E-mail address: a.goral@imim.pl (A. Góral).

https://doi.org/10.1016/j.apsusc.2018.06.102
Received 29 March 2018; Received in revised form 31 May 2018; Accepted 13 June 2018

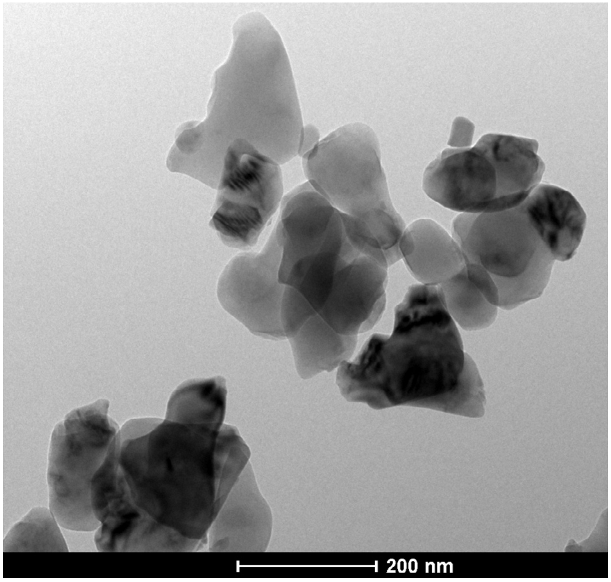

Fig. 1. Bright field TEM image of the α-Al_2O_3 powder.

mathematical relation between the amounts of Al_2O_3 nanoparticles added to the electrolytic bath and their concentration in the obtained coatings was examined. Additionally, the applied approach provides new solutions for the application of X-ray diffraction methods as non-destructive tools for determining deposit vacancy density, crystallographic texture and residual stresses.

2. Experimental and methodological procedure

2.1. Sample preparation

The Ni/Al_2O_3 coatings were electrodeposited with a potentiostat/galvanostat AUTOLAB model PGSTAT 302 from a Watts bath at a current density of 5 A/dm^2. The electrolytic bath consisted of 120 g/l $NiSO_4 \cdot 6H_2O$, 70 g/l $NiCl_2 \cdot 6H_2O$, and 50 g/l H_3BO_3, with various amounts of nano-sized alumina additions (20, 40, 60, 80 g/l). The grain size of the Al_2O_3 particles was in the range of 50–150 nm, Fig. 1. The process was conducted according to the following parameters: pH 4, temperature 40 °C, anode – a stationary nickel plate (99.9% purity), cathode – low carbon steel sheets as the substrate. The substrate was etched and ultrasonically cleaned before the experiment. Prior to the co-deposition process, the alumina particles were ultrasonically dispersed in the bath for 2 h and mechanically agitated (800 rpm) using a magnetic stirrer. During the co-deposition process, the plating bath was stirred by a magnetic stirrer with the stirring rate of 300 rpms and circulated with a peristaltic pump (50 rpm). After electrolysis, the samples were ultrasonically cleaned to remove any loosely adherent particles from the surface.

2.2. Microstructure analysis

Scanning and transmission electron microscopes (SEM: FEI E-SEM XL30, TEM: FEI TECNAI G2) were used in order to characterise the microstructures of the obtained coatings in both micro and nanoscale. The thin foils were prepared by means of the Focused Ion Beam (FIB) technique using the FEI QUANTA 3D Dual Beam. The percentage by volume (% vol.) of the Al_2O_3 nanoparticles incorporated in the deposit was determined with the use of the Loco's Shire program. Calculations of the alumina content incorporated into the Ni matrix were performed on the basis of analysis of ten areas of the SEM microstructure of the coating cross sections. The micrographs were performed in the mode of backscattered electrons (SEM BSE) to show the mass contrast of elements and identify the Ni and Al_2O_3 phases. The Loco's Shire program allowed to precisely isolate the areas of the Al_2O_3 phase and calculate its content in % vol.

2.3. Residual stress measurements

The residual stresses in the coatings were measured using non-destructive X-ray diffraction techniques (Bruker D8 Advance diffractometers with CoKα filtered radiation) by applying two methods; standard ω-$\sin^2\psi$, and GID-$\sin^2\psi$ method with grazing incidence X-ray diffraction geometry [25]. In the standard ω-$\sin^2\psi$ method, the measurement region is not strictly determined, as the irradiated volume changes during the measurement. Therefore the obtained results concerned the entire coating thickness, where stress gradients can be neglected. The GID-$\sin^2\psi$ method was applied to determine residual stresses in a well-defined surface layer with the appropriate thickness. Changing the beam incidence angle α allowed to calculate the residual stresses at a strict material penetration depth in the range of 0.9–5.0 µm ($\alpha \in 1$–6°) [25,26]. The residual stresses in the Ni-matrix phase were determined based on the {3 1 1} Ni reflection, 2θ = 114.9° in ω-$\sin^2\psi$ method and all Ni diffraction lines for the GID-$\sin^2\psi$ method. Diffraction elastic constants $1/2s_2 = (1+\nu)/E = 8.187 \cdot 10^{-6}\,\mathrm{MPa}^{-1}$ and $s_1 = -1.938 \cdot 10^{-6}\,\mathrm{MPa}^{-1}$ were used during calculations.

2.4. Determination of vacancy density and crystallographic texture

Micro-deformation fields, caused by crystal lattice defects i.e. vacancy density, were established using the ratio of the first and second order for I(1 1 1)/I(2 2 2) diffraction peak intensities, determined in Bragg-Brentano (BB) geometry. This ratio is independent from crystallographic texture compared to that measured for an annealed Ni powder, and is therefore a relative measure of the vacancies density.

The crystallographic texture was examined based on diffraction line intensity ratios recorded with symmetrical BB geometry, while peaks representing grain orientations with their {*hkl*} crystallographic planes parallel to the surface of the sample. The intensity ratio of the chosen peaks i.e. I200/I311, I(1 1 1)/I(3 1 1) and I(2 0 0)/{I(1 1 1) + I(2 0 0) + I(2 2 0) + I(3 1 1)} were taken into account and they were compared to the diffraction lines of Ni powder sample. Error of the ratios were established according to principle of error of quotient of two variables measured with the intensity error $\pm\sqrt{I(hkl)}$.

The relative texture coefficient $P_j(hkl)$ was determined, as follows:

$$P_j(hkl) = \frac{I_s(hkl)/I_p(hkl)}{\sum_{i=1}^{4} I_s(hkl)/I_p(hkl)} \quad (1)$$

where $I_s(hkl)$ and $I_p(hkl)$ are the intensities of diffraction peaks measured in the diffractogram of the deposit and the standard Ni powder with randomly oriented grains, respectively.

An additional procedure described by Morris [27], common for an inverse pole figure analysis was also applied i.e.:

$$P_M(hkl) = \frac{I_s(hkl)/I_p(hkl)}{\sum_{i=1}^{n} A_{hkl} I_s(hkl)/I_p(hkl)} \quad (2)$$

where A_{hkl} – Morris factor calculated from the division of spherical triangle ({1 0 0}-{1 1 0}-{1 1 1}) into a number of considered diffraction peaks (n).

The measured lattice parameter of the Ni matrix was calculated from the diffraction patterns obtained using the BB geometry in the direction perpendicular to the sample surface. The relatively high intensity {3 1 1} diffraction line was used to lattice parameter measurements and by differentiation of Bragg equation the error was calculated.